

VLBI STUDIES OF AURORAL KILOMETRIC RADIATION AND SOLAR TYPE III BURSTS USING THE WIDEBAND DATA PLASMA WAVE INSTRUMENT

R. L. Mutel, D. A. Gurnett, R. L. Huff

Dept. Physics & Astronomy, University of Iowa, Iowa City, IA 52242, 319-335-1950, FAX: 319-335-1753,
rlm@astro.physics.uiowa.edu

ABSTRACT

We discuss the feasibility of using the Wideband Data Plasma Instrument (WBD) for very long baseline interferometric (VLBI) studies of the location, size, and motions of terrestrial auroral kilometric radiation (AKR), solar Type III bursts, and Jovian hectometric radiation using multiple Cluster spacecraft. Previous investigations with similar instruments demonstrate that the intensities and brightness temperatures of these emissions may be suitable for VLBI detections using the WBD instrument. The main technical challenges are maintaining overall phase coherence of the system, precise a priori determination of spacecraft locations and velocities, and the difficult logistic requirement for real-time data acquisition of all four spacecraft near apogee. Assuming a total delay uncertainty of ~ 10 microseconds on each baseline and successful fringe detection on all six baselines, the instantaneous angular position of a source can be determined to an uncertainty of 10 arcmin. This corresponds to a position uncertainty of 375 km for an AKR source near the Earth. Measurement of source motion depends on phase stability of the system; a preliminary calculation indicates that the projected speed of an AKR source can be determined with an uncertainty of 50 m/sec.

1. INTRODUCTION

The Cluster mission provides a unique opportunity to study a variety of solar system radio sources using a four element very long baseline interferometer (VLBI) array. The VLBI technique, which has been used in centimeter wavelength radio astronomy since the late 1960's, involves simultaneous measurement of the complex coherence on a variety of baselines which are physically independent but which maintain phase coherence using highly stable local oscillators at each antenna. Ground-based VLBI data are usually recorded on magnetic tape for later correlation using a specialized hardware correlator.

In this paper we discuss the technical and scientific challenges involved in using the low frequency radio

receivers of the Wideband Data (WBD) plasma instrument on Cluster. In the optimal mode, we will send data from all four spacecraft to ground tracking stations in real time, and later correlate each pair of data streams using a software correlator. By analyzing the correlation amplitude, we can estimate the source size and structure. Measurement of the correlation versus delay for each baselines provides a sensitive measure of the angular location of the source. Since the sensitivity of the WBD system is relatively low, we can only study the most intense low-frequency radio sources in the solar system.

2. INTERFEROMETRIC DELAY-RATE MAPPING OF SOURCE LOCATION

A simple two element interferometer separated by distance $\vec{\sigma}$ measures the mutual coherence of a signal arriving from direction \vec{n} over a projected separation $\vec{\sigma} \cdot \vec{n}$. There is a geometrical delay τ between the arrival of the wave front at the far element relative to the near element (Fig. 1)

$$\tau = \frac{1}{c} (\vec{\sigma} \cdot \vec{n}) \quad (1)$$

This delay can be determined by maximizing the cross-correlation amplitude between data streams from pairs of antennas using a variable delay offset. The locus of source locations for a given delay is a great circle on the celestial sphere in a plane orthogonal to the arrival direction of the wavefront. For a multi-element interferometric array, each pair of elements can be used to measure an independent geometrical delay. The resulting great circles will intersect at a unique location on the celestial sphere, providing an estimate of the source location. The uncertainty in each delay measurement is

$$\delta\tau_{obs} = \frac{1}{c} (\delta\vec{\sigma} \cdot \hat{n} + \vec{\sigma} \cdot \delta\hat{n}) + \delta\tau_{clock} \quad (2)$$

Assuming normal orientation of the baseline to line of sight and solving for the source angular position uncertainty, we obtain

$$\delta\theta \approx \frac{c\tau_{clock}}{\sigma} + \frac{\delta\sigma}{\sigma} \quad (3)$$

In the real-time data acquisition mode (TDA Mode 8), the WBD telemetry from each Cluster spacecraft is transmitted directly to a NASA Deep Space Network downlink antenna where it is time stamped to very high accuracy (<10 μsec) using hydrogen maser clocks. The uncertainty in spacecraft separation is likely to be ~ 1% of the separation (Escoubet *et al.* 1997). These are comparable contributions at separations ~1,000 km and result in a source position uncertainty $\delta\theta \sim 10^{-3}$ radians (3 arcmin) at 1,000 km projected baseline length. This corresponds to a source position uncertainty $\delta x \sim 130$ km when the Earth is viewed from apogee (19.6 R_E).

For narrowband emission, such as most AKR emission, the delay uncertainty can be dominated by the width of the correlation peak, given by the reciprocal bandwidth of the emission. For example, a source bandwidth of 1 KHz, results in a delay uncertainty of 1 millisecond, much greater than the uncertainties caused by geometric and electronics uncertainties discussed above. For this case, the uncertainty in angular position is minimized by using the longest baselines. For example, an apogee separation of 3 R_E (possible configuration for second year, Escoubet *et al.* 1997) results in an angular uncertainty of 0.9 degrees, or 0.3 R_E at the Earth.

3. AKR STUDIES

Auroral kilometric radiation (AKR) is the most intense terrestrial electromagnetic radiation. It is associated with discrete auroral arcs and has a maximum radiated power exceeding 10^9 W (Gurnett 1974). AKR emission typically extends from 50 to 500 KHz, and is highly polarized in the right-hand extraordinary (R-X) mode, although a small fraction (~2 percent) is L-O mode (Shawhan and Gurnett 1982). The emission is often

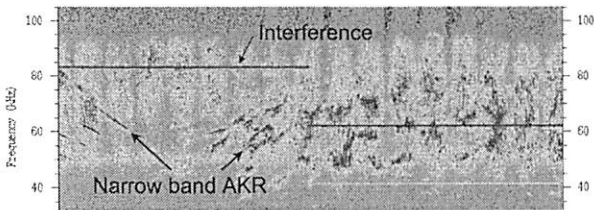


Fig. 1. AKR emission showing drifting narrow-band frequency structure.

narrow-band and rapidly drifting in frequency (Fig. 1). *In situ* satellite observations of the source emission region (e.g. Ergun *et al.* 1998) show that the emission

arises in density depleted cavities with a ratio of electron plasma to cyclotron frequency

$$\frac{\omega_{pe}}{\omega_{ce}} \leq 0.2 \quad (4)$$

The emission is thought to result from a cyclotron maser mechanism in which electrons interact with waves via a Doppler-shifted cyclotron resonance condition. A loss-cone electron distribution provides the free energy source (Melrose 1973; Wu and Lee 1979).

Although AKR emission has been extensively studied since its discovery in 1964 (Benediktov *et al.* 1965), only a few observations have been able to directly

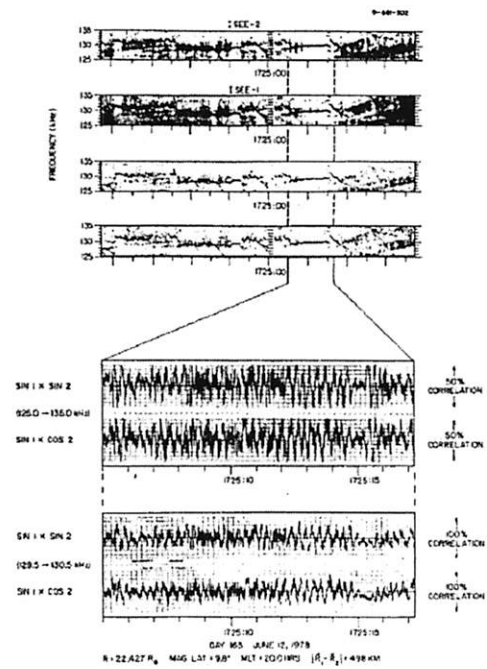


Fig 2. Fringe detection of narrow-band AKR emission from ISEE-1 and 2 VLBI observations on 12 June 1978 (Baumbeck 1986).

address the question of source location and motion within the magnetosphere. Kaiser and Alexander (1976) used the RAE-2 spacecraft to observe lunar occultations of AKR emission at 250 KHz. They found that most emission arose above the polar regions at a radial distance of 2-3 R_E . They also found considerable evidence for multiple sources and source motion on a timescale of tens of minutes. Huff *et al.* (1988) combined DE-1 images of the auroral oval along with AKR observations from the plasma wave instrument (PWI). The PWI instrument allowed for 2-dimensional direction finding by determining the direction of null patterns as the 200m PWI dipole rotated with

spacecraft spin. Huff et al. mapped the null directions to magnetic field lines high above bright auroral spots, with the higher frequencies arising at lower altitudes (Fig. 3).

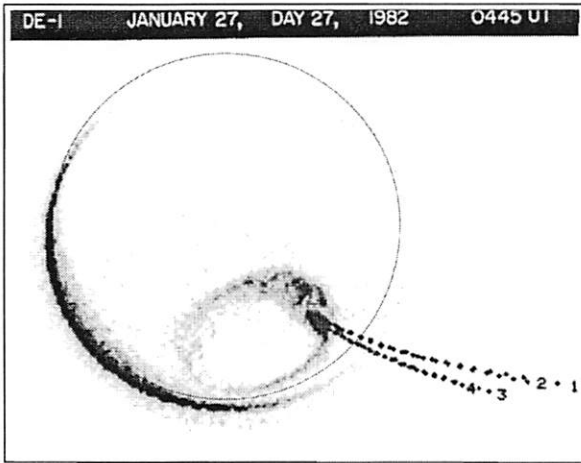


Fig. 3. Location of AKR emission on field lines above auroral bright spots (from DE-1, Huff et al. 1988). The dashed lines show magnetic field lines through the bright spot and inferred AKR source locations at 104 KHz (1), 136 KHz (2), 170 KHz (3), and 218 KHz (4).

Using VLBI on Cluster, we will be able to directly measure for the first time the three-dimensional angles of arrival of AKR emission and map them to the auroral field lines. Since multiple AKR sources are likely to be active simultaneously, it will be important to have all six baseline delays measured to map the different source locations as a function of frequency channel.

4. SOLAR TYPE III RADIO BURST STUDIES

Solar type III bursts originate when energetic electrons ($\sim 1-10$ keV) are accelerated in solar active regions and travel outward through the solar corona. The electron beams excite electrostatic plasma oscillations (Langmuir waves) at the local plasma frequency ω_p . Some of this energy is converted into electromagnetic waves at both ω_p and $2\omega_p$ via non-linear wave-particle interactions. As the source region propagates into regions of lower electron density the observed frequency drifts downward as expected (Fig. 4). Since the flux density of Type III bursts near the Earth is very large (comparable with most intense AKR emission), they are easily detected with the WBD instrument and are a natural target for VLBI studies.

Unfortunately, it is not clear that VLBI observations of Type III bursts will be successful, since the observed source size is likely to be much larger than the angular resolution of the interferometer. Previous studies of Type III bursts demonstrate that observed source size

and location are dominated by refraction and scattering both from electron density fluctuations and possibly neutral current sheets in the intervening interplanetary medium. For example, scattered-broadened sizes at

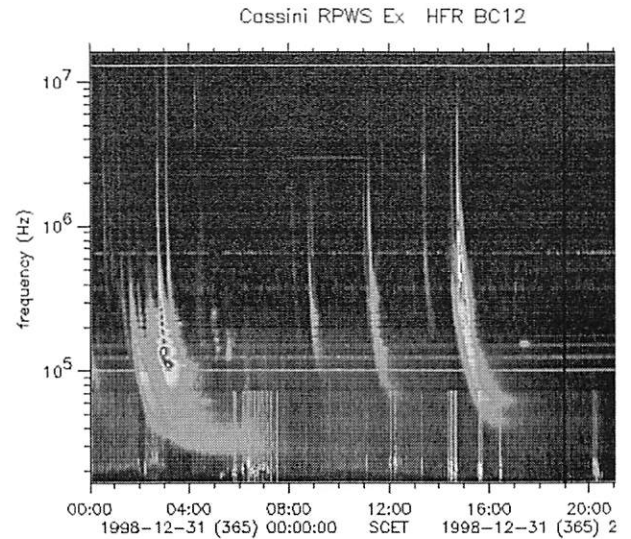


Fig. 4. Solar Type III bursts observed by Cassini spacecraft on 31 Dec 1998. Note downward frequency drift caused by outward motion of source to regions of lower density.

frequencies between 100 and 500 KHz have been deduced indirectly by simultaneous two-spacecraft observations by Lecacheux et al. (1989). They find that source sizes range from 10 to 35 degrees, compared with the 1 to 10 arcmin angular resolution for typical Cluster VLBI baselines at the same frequencies. However, there are two possible mitigating factors which may allow VLBI detections. The first is as the source travels close to the Earth, the intervening scattering screen becomes thinner, so that the total scattering size decreases. Spangler and Sakurai (1995) used VLBI to measure the phase scintillation spectra of several extragalactic radio sources whose lines of sight passed close to the Sun. Assuming a power-law form for the spatial spectrum of density irregularities, they determined the strength of interplanetary scattering as a function of radial distance from the Sun

$$C_n^2(r) = 1.8 \cdot 10^{10} \left(\frac{r}{10r_{sun}} \right)^{-3.7} m^{\frac{20}{3}} \quad (5)$$

We have used this expression to calculate the scattered-broadened angular size as a function of observer-source distance (ξ , a.u.) and frequency (ν , MHz):

$$\theta_{scat}(\xi, \nu) = 1.1^\circ \cdot \left[(1 - \xi)^{-2.7} - 1 \right] \cdot \nu^{-2.2} \quad (6)$$

For small source-observer distances (less than 0.01 au or $\sim 10^6$ km) the source size is comparable with the interferometer fringe spacing, so that it may be possible to study the size and motion of Type III sources as they pass close to the Earth. The second point is that the scatter-broadened image may not be a perfectly smooth diffractive brightness profile, but may contain at least some fractal 'scintiles' with very small angular sizes. This can occur if the spatial power spectrum of density fluctuations is 'steep' i.e., has an index greater than 4.0 (Goodman and Narayan 1985). Although there is ample evidence for a Kolmogorov (11/3) spectrum in the interplanetary medium (e.g. Woo & Armstrong 1989), there may be localized regions which contain steeper power-law turbulence. Since the flux density from Type II bursts is very intense (often exceeding $>1000:1$ signal-to-noise ratio), even if $\sim 1\%$ of the scattered radiation is scattered from such regions, it may be possible to detect the source using VLBI and hence to study both the physics of the Type II bursts and the intervening turbulence.

5. JUPITER HECTOMETRIC RADIATION

Low frequency ($f < 1$ MHz) radio emission from Jupiter was first detected by the Voyager Planetary Radio Astronomy instrument in April, 1978 (Desch and Kaiser 1980). There are apparently two types of Jovian kilometric radiation (KOM), broadband (bKOM) and narrowband (nKOM). The bKOM emission is highly circularly polarized, extends from ~ 20 KHz to at least 1 MHz, and has a strong dependence of Jupiter's central meridian longitude (CML). The average equivalent isotropic radiated power is $3 \cdot 10^8$ W (Alexander et al. 1981), although a peak power of $5 \cdot 10^9$ W has been detected about 1% of the time (Desch and Kaiser 1980). The nKOM emission (Kaiser and Desch 1980) occurs between 50 and 180 KHz in events that typically last for a few hours or less. Bandwidths of 40-80 KHz are common. The peak power can reach 10^9 W, but is more typically 10^8 W. Like bKOM emission, there is a CML dependence on the probability of emission, but with a period that is slightly larger than the CML period (Kaiser and Desch 1980).

The precise location of both nKOM and bKOM radio emission is uncertain, but both are very likely located within the Io plasma torus. As viewed from the Cluster spacecraft at 1 a.u., the Io plasma torus has an angular diameter of ~ 2 arcmin. If the WBD instrument could detect Jovian KOM emission, it would provide an excellent absolute calibration of the delay mapping technique, since the source location is very well determined. In addition, it may be possible to distinguish between source locations close to Jupiter and those near Io since in the latter case the source will move ~ 2 arcmin over the orbital period of Io (42 hr).

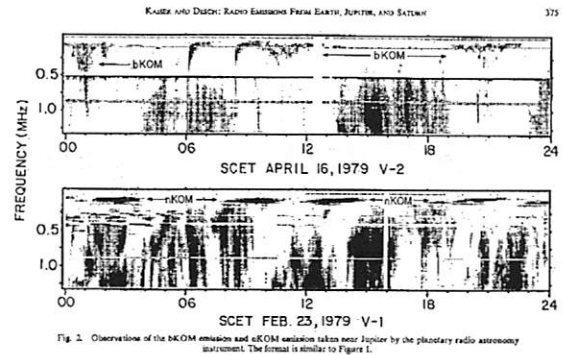


Fig. 5. Observations of the bKOM emission and nKOM emission taken near Jupiter by the planetary radio astronomy instrument. The format is similar to Figure 1.

Fig. 5. Jovian kilometric radiation spectra observed with the PRA instrument aboard Voyager 2 (Kaiser and Desch 1984). Both broadband (bKOM, top panel) and narrow band (nKOM, bottom panel) radiation can be seen.

The most significant technical challenge will be whether the WBD receiver sensitivity is adequate to detect Jovian emission at 1 a.u. The noise floor of the WBD instrument has been measured in the laboratory to be $\sim 1.5 \cdot 10^{-17}$ V² m⁻² Hz⁻¹ between 125 and 500 KHz (Gurnett, priv. comm.). This corresponds to a smallest detectable flux density $S \sim 3 \cdot 10^{-20}$ W m⁻² Hz⁻¹, or a minimum detectable radiated power (equivalent isotropic) of $2 \cdot 10^5$ W Hz⁻¹ at Jupiter. Assuming a emission bandwidth of 50 KHz, this means the minimum integrated power is $P \sim 5 \cdot 10^9$ W, which is comparable to only the most luminous Jovian nKOM and bKOM bursts. Since VLBI mode observations will occur only infrequently it appears unlikely that we will be fortunate enough to be observing in VLBI mode during the most intense KOM outbursts.

6. TECHNICAL AND OPERATIONAL REQUIREMENTS FOR CLUSTER VLBI

There are several technical and operational requirements that must be met to allow scientifically meaningful VLBI observations using the WBD receivers on Cluster. The most critical technical challenge is adequate phase stability through the entire data acquisition, downlink, and recording paths of each spacecraft. The overall RMS phase jitter over a single coherent integration time (typically 1-3 sec) must be at least as small as

$$\sigma_{\phi} = \frac{1}{2} \cdot \frac{2\pi}{\Delta\nu} = \frac{\pi}{\Delta\nu} \quad (7)$$

where $\Delta\nu$ is the largest bandwidth used. This could be as large as 77 KHz, so the short-term phase jitter must be less than 40 μ sec to allow coherent cross-correlation of signals from separate receivers. A perhaps more severe requirement is that the phase of independent

local oscillator chains (including downlinks) be sufficiently stable that the interferometer phase can be unambiguously determined over an entire 'scan', i.e. the duration of an event. For example, in the case of AKR emission, this might be the lifetime of an individual emission region as it evolves along a magnetic field line, which could be as long as a few minutes. Adopting a nominal criterion of 0.5 radians maximum phase uncertainty in the scan interval, we require so that the overall fractional frequency stability needs to be at least

$$\frac{\delta\nu}{\nu} \leq \frac{1}{4\pi} \cdot \frac{40\mu\text{sec}}{200\text{sec}} \approx 2 \cdot 10^{-8} \quad (8)$$

This should be easily satisfied since the WBD receiver is phase locked to the on-board Cluster master oscillator ('Ultra-Stable Oscillator') which has a fractional frequency stability of 10^{-9} over 12 hours (Gurnett, Huff & Kirchner 1997).

As discussed in §2, another requirement is that the positions and separations of the Cluster spacecraft must be known with sufficient accuracy to allow delay mapping of source positions. In addition, it will be far easier to build a correlator geometry model if uncertainties in baseline length and orientation can be separated from source motion effects. The nominal uncertainty of 1% of the separation quoted by Escoubet et al. (1997) should be adequate for most VLBI observations, at least until the uncertainty in separation becomes comparable with the observing wavelength.

Finally, it is convenient that the data streams from all four spacecraft have time stamps that are accurate to at least the inverse observing bandwidth. As discussed above, this means an absolute accuracy of 40 μsec , although somewhat larger time errors could be accommodated in principle by a more thorough fringe search in the correlator. In VLBI mode, the WBD data streams will be transmitted directly to Deep Space Network ground stations ('real-time' data acquisition), which time stamp each data stream with a UT stamp derived from on-site atomic clocks. The time stamps should be accurate to 1 μsec or less, so data stream time alignment should not be a problem.

A summary table of the technical requirements for VLBI science with the WBD instrument is given below.

Table 1. Technical requirements for VLBI observations using the Cluster WBD instrument .

Parameter	Tolerance
Short term phase jitter	< 40 μsec
Absolute Time Synchronization Error	< 40 μsec
Local oscillator frequency stability (fractional, 300 sec)	< $2 \cdot 10^{-8}$
Spacecraft position uncertainty (RMS)	< 1 km
Minimum Detectable Flux density (5σ detection)	> $3 \cdot 10^{-20} \text{ W m}^{-2} \text{ Hz}^{-1}$

An important but potentially problematic logistic challenge will be securing sufficient DSN resources to track all four Cluster spacecraft simultaneously. In the early stages of the mission (when the spacecraft are relatively close), it may be possible to use a single downlink antenna to acquire data in real time from all spacecraft, at least near apogee. However, as the spacecraft drift farther apart, it will require multiple DSN antennas to acquire the data. This will likely severely limit the time available for VLBI observations. We therefore expect that we will emphasize VLBI science studies relatively early in the mission.

REFERENCES

- Alexander, J.K., *et al.* 1981, J.G.R. 86, 8529.
 Benediktov, E. A. *et al.* 1965, Cosmic Res. 3, 492.
 Desch, M. D. and Kaiser, M. L. 1980, J.G.R. 85, 4248.
 Ergun, R. E. *et al.* 1998, G.R.L. 25, 2061.
 Escoubet, C. P., Schmidt, R., and Goldstein, M. L. 1997, Sp. Sci. Rev. 79, 11.
 Goodman, J. J., & Narayan, R. 1985, M.N.R.A.S. 214, 519.
 Gurnett, D. A. 1974, J.G.R. 79, 4227.
 Gurnett, D.A., Huff, R. L., & Kirchner, D. L. 1997, Sp. Sci. Rev., 79, 195.
 Huff, R. L., *et al.* 1988, J.G.R. 93, 11445.
 Kaiser, M. L. and Alexander, J. K. 1976, G.R.L. 3, 37.
 Kaiser, M. L. and Desch, M. D. 1980, J.G.R. 7, 389.
 Lecacheux, A., Steinberg, J-L., Hoang, S. & Dulk, G. 1989, Astr. Astroph. 217, 237.
 Melrose, D. B. 1973, Aust. J. Phys., 26, 229.
 Shawhan, S.D. and Gurnett, D. A. 1982, G.R.L. 9, 913.
 Wu, L. C. & Lee, L. C. 1978, Ap. J. 230, 621.